Quantifying the relation between bond number and myoblast proliferation†

Tanyarut Boontheekul,‡[ab] Hyun-Joon Kong,[b] Susan X. Hsiong,[ab] Yen-Chen Huang,[c] L. Mahadevan,[b] Herman Vandenburgh[d] and David J. Mooney*[b]

Received 4th January 2008, Accepted 15th January 2008
First published as an Advance Article on the web 9th April 2008
DOI: 10.1039/b719928g

Many functions of the extracellular matrix can be mimicked by small peptide fragments (*e.g.*, arginine–glycine–aspartic acid (RGD) sequence) of the entire molecule, but the presentation of the peptides is critical to their effects on cells. It is likely that some effects of peptide presentation from biomaterials simply relate to the number of bonds formed between cell receptors and the adhesion ligands, but a lack of tools to quantify bond number limits direct investigation of this assumption. The impact of different ligand presentations (density, affinity, and nanoscale distribution) on the proliferation of C2C12 and human primary myoblasts was first examined in this study. Increasing the ligand density or binding affinity led to a similar enhancement in proliferation of C2C12 cells and human primary myoblasts. The nanoscale distribution of clustered RGD ligands also influenced C2C12 cells and human primary myoblast proliferation, but in an opposing manner. A rheological technique and a FRET technique were then utilized to quantify the number of receptor–ligand interactions as a function of peptide presentation. Higher numbers of bonds were formed when the RGD density and affinity were increased, as measured with both techniques, and bond number correlated with cell growth rates. However, the influence of the nanoscale peptide distribution did not appear to be solely a function of bond number. Altogether, these findings provide significant insight to the role of peptide presentation in the regulation of cell proliferation, and the approaches developed in this work may have significant utility in probing how adhesion regulates a variety of other cellular functions and aid in developing design criterion for cell-interactive materials.

1. Introduction

A variety of approaches have been developed to functionalize material surfaces with bioactive components to gain a greater control over the cell response to the materials. Functionalizing with short peptide sequences derived from extracellular matrix

[a]*Department of Chemical Engineering, University of Michigan, Ann Arbor, MI, 48109, USA*
[b]*School of Engineering & Applied Sciences, Harvard University, 29 Oxford St, Pierce Hall Rm. 325, Cambridge, MA, USA. E-mail: mooneyd@seas.harvard.edu; Tel: +617-384-9624*
[c]*Deptartment of Bioengineering, Massachusetts Institute of Technology, Cambridge, MA, 02139, USA*
[d]*Department of Pathology, Brown Medical School, Providence, RI, 02906, USA*

† The HTML version of this article has been enhanced with colour images.
‡ Present address: Institute of Bioengineering and Nanotechnology, 31 Biopolis Way #04-01, Nanos, Singapore 138669.

molecules (*e.g.*, the arginine–glycine–aspartic acid [RGD] sequence of fibronectin), in particular, has been extensively investigated,[1] including targeting drugs to tumor vasculature,[2] and novel design of biomimetic materials for tissue engineering.[3] For the latter application, the RGD motif has been incorporated into polymers to trigger cell adhesion and subsequently control tissue regeneration, including bone and neural regeneration.[4,5]

Cell adhesion peptides may be presented in a variety of manners from biomaterials, and critical variables include the density of peptides, their affinity for cellular receptors, and their nanoscale distribution. The density of peptides likely will alter the number of bonds formed with cellular receptors, and activation of intracellular signaling pathways.[3] The peptide affinity (*e.g.*, cyclic *versus* linear RGD peptides[6]) may also impact bond formation. Following integrin occupancy, integrin clustering is required to elicit many cellular responses,[7] and clustering of adhesion ligands on a biomaterial may result in more efficient clustering of receptors as compared to a uniform distribution.[8] These variables in peptide presentation have been demonstrated to control the adhesion, proliferation, and differentiation of various cell types, including fibroblasts, chondrocytes, osteoblasts, myoblasts, endothelial, smooth muscle and neuronal cells, both *in vitro* and *in vivo*.[4,9–13] However, while it is widely assumed that the number of bonds that form between cell receptors and adhesion ligands underlie at least part of this control, a lack of assays to quantify bond number has limited direct testing of this assumption. Quantification of receptor–ligand binding is a primary concept for pharmacology[14] and can be readily performed with soluble radiolabeled ligands,[15,16] but not immobilized ligands, particularly when the cells are immobilized within a three-dimensional material. More recently, fluorescence correlation spectroscopy (FCS) has provided a means to examine this issue in living cells, but this computationally-intense approach only allows a small number of cells to be analyzed, and changes in cell position during analysis can introduce errors.[14]

This study examined in a quantitative manner the relation between one important cell function, proliferation, and varying RGD peptide presentation from

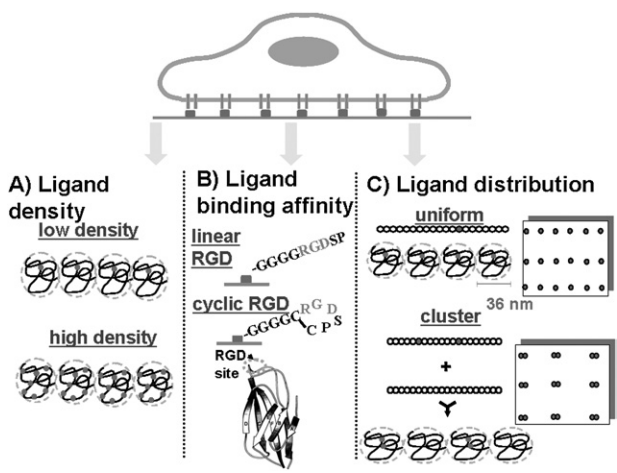

Fig. 1 Three different presentations of RGD ligand (●) to control cell–material interactions were investigated in this study. Ligand density (referred as degree of substitution, DS) is simply varied by altering the number of RGD ligands incorporated per polymer chain (A). Ligand binding affinity is enhanced by using cyclic RGD *versus* linear RGD. Cyclic RGD binds to integrin receptors with higher affinity as conformation of cyclic RGD more closely mimics a common structural motif for native RGD sites in fibronectin (FG loop) (B). Uniform ligand distribution can be achieved by mixing polymers containing ligands with others containing similar quantities of ligands (upper C). In contrast, simple mixing of RGD-containing polymers with unmodified polymers at an appropriate ratio allows one to decouple RGD distribution and RGD bulk density (lower C).

a biomaterial (Fig. 1). Alginate, a naturally-derived polysaccharide composed of linearly assembled (1–4)-linked β- mannuronic acid (M), and α-guluronic acid (G) monomers,[17] was utilized as the adhesion substrate in this study, as the lack of interaction between cells and native alginate allows it to act as a "blank slate". Cell adhesion to these gels can be promoted by incorporation of immobilized cell adhesion peptides (*e.g.* G4RGDSP) *via* carbodiimide chemistry.[4,18] Two types of skeletal muscle cells were employed in this study: C2C12 cells and human primary myoblasts. The transformed C2C12 cells, originally derived from mouse myoblasts, have been widely used in studies of muscle biology and regeneration.[19] However, cell lines typically lose some sensitivity to environmental cues, specifically those related to adhesion. To address this concern, experiments were also performed with human primary myoblasts to most closely approximate normal human muscle biology. In the second series of studies, the formation of receptor–ligand bonds as a function of peptide presentation was quantified with two different approaches: rheological measurements and a FRET technique. The viscoelastic properties of mixtures of RGD-containing alginate and cells were measured, as receptor–peptide bond formation leads to changes in viscoelastic properties.[20] FRET is a technique used to measure the interactions between two molecules labeled with two different fluorophores (donor and acceptor) by the transfer of energy from the excited donor to the acceptor,[21,22] and has recently been demonstrated to allow for quantification of bond number between cells immobilized in RGD-presenting biomaterials.[23] Finally, the correlation between the growth rates of the C2C12 cells and human primary cells and the number of bonds formed between cells and the various gels was examined.

2. Materials and methods

2.1 Material chemistry

Oligopeptides (linear-GGGGRGDSP, linear-GGGGRGDASSK, or cyclic-GGGG[CRGDSPC], Commonwealth Technology, VA) were covalently conjugated to sodium alginates rich in GG-block (MVG, Pronova, Norway, $M_w = 2.7 \times 10^5$ g mol^{-1}) using carbodiimide chemistry.[18] The number of peptides per single polymer chain, referred to as degree of substitution (DS), was varied up to three orders of magnitude by changing the amount of peptides added in the reaction (16.7 linear mg peptide per g alginate or 3.4 mmol peptide per mol alginate yields DS = 2 while 167.0 mg linear peptide per g alginate was equal to DS 20, and so on). The modified alginates (except GGGGRGDASSK-containing alginate) were reconstituted in calcium-free DMEM (Invitrogen) to obtain 2% w/v solution prior to gelation. Maintenance of ring closure for cyclic oligopeptides following this coupling reaction was confirmed, as there was no free sulfur detected by DTNB assay.

GGGGRGDASSK-containing alginate was further coupled with 5-(and-6) carboxyltetramethylrhodamine succinimidyl ester (Molecular Probes, cat. #C1171) for FRET experiments. Briefly, RGD-modified alginates were dissolved in 0.1 M sodium bicarbonate buffer at pH 8.5. 5(and 6)-Carboxyltetramethylrhodamine succinimidyl ester was then added to the solution, followed by 1-ethyl-3-[3-(dimethylamino)propyl]carbodiimide (EDC). The molar ratio of oligopeptide: fluorescent probes: EDC was kept constant at 1 : 1.2 : 5. After a 24-hour reaction, the solution was dialyzed, sterilized, lyophilized, and reconstituted in Phenol-Red-free medium (Invitrogen) to obtain 1% w/v fluorescently-labeled alginate solution.

2.2 Alginate hydrogel formation

To form hydrogels for *in vitro* cell studies, 2% (w/v) alginate solutions were mixed with autoclaved $CaSO_4$ slurry (0.41 g $CaSO_4$ per ml ddH_2O, ratio of 40 μl $CaSO_4$ slurry to 1 ml alginate) through a syringe connector to facilitate the mixing process and prevent entrapment of air bubbles during mixing. The resulting mixture was cast between two glass plates separated with 1 mm spacers and allowed to gel for

30 minutes. Gel disks were punched out using a 11.1 mm puncher, and incubated in medium overnight prior to use. Typically, a single type of alginate was utilized to form gels, leading to uniform ligand distribution. In certain experiments to vary RGD ligand distribution, non-modified alginates were mixed with RGD-modified alginates at different mixing ratios prior to mixing with calcium slurry to form gels.[24] For example, 10 times dilution of RGD-modified alginates (*e.g.*, 9 parts of unmodified alginates with one part of RGD-modified alginates at DS 20) created a cluster of RGD islands, while the bulk density was identical to solely using DS 2 RGD-modified alginates to create gels. In this study, three different RGD distributions were prepared: (1) uniform distribution (single type of DS 2, RGD spacing = 36 nm); (2) cluster organization of (DS20/DS0) = (1/9) (RGD spacing = 85 nm); and (3) cluster organization of (DS40/DS0) = (1/19) (spacing = 121 nm). Island spacing was calculated as previously described.[25] In this paper, the notation of these RGD distributions is presented as X RGDs/Y nm, where X refers to the number of peptides per single polymer chain as a local density and Y refers to the distance between clusters or spacing. These three different RGD presentations are denoted as: (1) 2 RGDs/36 nm (2) 20 RGDs/85 nm (3) 40 RGDs/121 nm, respectively.

2.3 *In vitro* cell studies

Two myoblast cell types were used in this study: C2C12 mouse myoblast cell line (ATCC passage number 7–15) and cryopreserved primary adult human skeletal muscle cells. Human primary cells (average purity = 80% myoblasts) were isolated from biopsies of the Vastus lateralis of healthy male adults aged 35–48; the detailed procedure is described in Powell *et al.*[26] Cells were cultured in growth media and maintained subconfluent prior to each experiment. Media was changed daily to prevent myoblast differentiation. The growth medium of C2C12 cells was DMEM supplemented with 10% FBS, 1% penicillin–streptomycin (Invitrogen). The growth medium of human primary cells was basal skeletal muscle medium SkGM with supplement kit (Cambrex, cat. #CC-3160), as adapted from Powell *et al.*[27] Cells were seeded at approximately 10 000 cells cm^{-2} onto alginate disks placed in non-tissue-culture treated 24 well plates. At 4 hour post-seeding, non-adherent cells were removed and the alginate gels were transferred to new plates. Alginate disks (at least 4 samples per condition per time point) were harvested at 4 hours and days 1, 2, and 3 for C2C12 cell lines and at 4 hours and days 1, 3, 5, 8 for human primary cells. Samples were placed in 1 ml of 0.25 M trypsin for 5 minutes at 37 °C, to which 9 ml of 50 mM EDTA in phosphate buffered saline (PBS) pH 7.4 was subsequently added and incubated for 30 minutes in order to dissolve the alginate gels. Cell number was determined using a Coulter counter (Beckman Coulter, model Z2). Media was changed daily during the experiments.

2.4 Rheological measurements in cell-crosslinking system

The viscoelastic properties of cell–alginate mixture were determined with a cone-and-plate rheometer (C-VOR 120 Bohlin instrument, 20 mm diameter, 4° cone angle) to examine the receptor–ligand interactions. To prepare the mixture, a cell pellet was mixed with 2% (w/v) RGD-containing alginate through a syringe connector to yield a final concentration of 150×10^6 cells per ml mixture. The resulting mixture was incubated at 37 °C for 30 minutes prior to testing. RGD-Modified alginates tested in this study were alginates containing linear G_4RGDSP at DS = 0, 2, 4, 20, 40, cyclic G_4CRGDSPC at DS = 2, 20, and the mixture of linear G_4RGDSP at (DS20/DS0) = (1/4) (20 RGDs/58 nm) and (DS40/DS0) = (1/9) (40 RGDs/85 nm). The oscillatory regime of a controlled stress rheometer was used to measure storage (G') and loss (G'') moduli of the alginate solutions in the absence or presence of cells as a function of frequency in the range from 0.01–10 Hz. The testing temperature was varied from 4, 10, 25, to 37 °C. The stress amplitude was fixed at 0.05 Pa,

as it was within the linear viscoelastic region when testing in an amplitude sweep at constant frequency 1 Hz. The gap opening at the apex of the cone and plate was fixed at 150 μm and the temperature control was achieved within ±0.1 °C. The same experiment was repeated with blocking of cell receptors with RGD-modified alginate solutions prior to mixing to confirm specificity of this receptor–ligand binding. Cell receptors were blocked by incubating cells for 30 minutes with soluble G_4RGDSP ligands at the concentration of 5 mM. Gap size dependence of G' and G'' as a function of time was examined by testing the samples with a plate-and-plate rheometer. The gap size between plates was varied from 50, 100, to 250 μm at 25 °C.

In order to calculate the number of crosslinks between cell receptors and ligands, viscoelastic properties of the cell–alginate mixture determined at varying temperatures (4, 10, 25, and 37 °C) were next analyzed (an example is shown in Fig. 8A,B). Results from temperature dependence assays were utilized to calculate zero-shear viscosity (η_0), in order to further calculate horizontal shift factors (a_T) and activation energy required to dissociate the receptor–ligand bonds ($\triangle\mu$). Zero-shear viscosity (η_0), estimated from $\eta_0 = \lim_{\omega\to 0} G''/\omega$, was used to calculate the horizontal shift factors (a_T) at each temperature using eqn (1) and the reference temperature (T_0) was assumed to be 25 °C.

$$\eta_0(T) = \lim_{\omega\to 0}\frac{G''(T,\omega)}{\omega} = \lim_{\omega\to 0}\frac{G''(T_0,a_T\omega)}{\omega} = \eta_0(T_0)a_T\omega = a_T\eta_0(T_0)^{28} \quad (1)$$

The plot between reduced frequency (products of a_T and frequency) *versus* G' or G'' was shown to confirm that the horizontal shift factor could be employed to shift the curves of each temperature to form one master curve (an example is shown in Fig. 8C).[28]

The activation energy ($\triangle\mu$) was next calculated from the slope obtained by fitting the horizontal shift factors (a_T) and the reciprocity of temperatures from the relation in eqn (2).

$$\tau_{\text{disso}} = \Omega_0^{-1}e^{\triangle\mu/kT}\ ^{28} \quad (2)$$

where $\triangle\mu$ is the free energy to dissociate the bond (J), k is the Boltzmann constant (J K^{-1}), and T is absolute temperature (K), see the inserted plot in Fig. 8C.

To calculate the number of crosslinks between RGD ligands and cell receptors from the activation barrier energy obtained from rheological measurements, the value of the binding force between linear RGD and cell receptors was adopted from a study of interactions between osteoblasts and RGD ligands assessed by atomic force microscopy (AFM) ($f_{0,\ \text{linear}} = 3.20 \times 10^{-11}$ N).[29,30] The bond length used was 5 nm, a median value of separation distance.[31] Because a previous study has shown that the bond strength with cyclic RGD is higher than linear RGD, the bond strength between cyclic RGD and cell receptors was estimated by values from Lehenkari *et al.* and Xiao *et al.*[29,32] ($f_{0,\ \text{cyclic}} = 4.27 \times 10^{-11}$ N).

2.5 Fluorescent resonance energy transfer (FRET) to monitor an extent of receptor–ligand bond formation

FRET was utilized to measure the interactions between cell receptors (labeled with donor fluorophores—5-hexadecanoylaminofluorescein [Molecular Probes cat. #H110]) and RGD ligands (conjugated with Rhodamine as acceptor fluorophores as described earlier). C2C12 cell membranes were labeled overnight. Fluorescein was dissolved with DMSO and sterile-filtered prior to adding to cultured cells at the ratio of 1 mg per 15×10^6 cells. When testing, cells were trypsinized and counted. Each sample contained 1, 5, or 10×10^6 cells was mixed with 150 μl of 1% GGGGRGDASSK-Rhodamine-containing alginate solutions. Phenol-Red-free medium was added to obtain a total volume of 2 ml per sample. Samples were incubated in 5% CO_2, 37 °C with an orbital shaker for 10 minutes to prevent cell

sedimentation. Changes of emission from donor and acceptor fluorophores were examined with a fluorimeter (Fluoromax-3, Jobin Yvon), while exciting the solutions at 488 nm. Control conditions included emission from donor fluorophore labeled cells without the acceptor fluorophore, the emission from acceptor fluorophores coupled to RGD-ligands for each ligand presentation without the donor fluorophore, and the emission from donors and acceptors in the test samples when the receptors were initially blocked with soluble G_4RGDSP for 30 minutes. To analyze cell receptor–ligand interactions, the emission intensity of donors at 520 nm was used to calculate the degree of energy transfer (ψ) by comparing the yield of donor emission in the presence (Φ_{green}) and absence of acceptor ($\Phi_{green,0}$) by using eqn (3).

$$\psi = 1 - [\Phi_{green} / \Phi_{green,0}]^{21} \quad (3)$$

2.6 Radiolabeling of G_4RGDASSKY to monitor extent of receptor–ligand bond formation in solution

G_4RGDASSKY oligopeptides (Commonwealth Biotechnology Inc., VA) were linked with ^{125}I (Perkin Elmer, 0.74 μCiug^{-1}).[23] Briefly, the iodinated oligopeptides were coupled to sodium alginate using previously-described aqueous carbodiimide chemistry. The molar ratio of oligopeptides to sugar residues was varied from 0.0015 : 1 to 0.03 : 1. The number of ^{125}I-G_4RGDASSKY was first calibrated to the radioactivity using a gamma counter. The amount of ^{125}I-G_4RGDASSKY-alginate bound to cells was then measured by mixing a suspension of cells (cell density: 20 000 cells per ml) with ^{125}I-G_4RGDASSKY-alginate solution at varied polymer concentrations. The number of RGD peptides linked to a single alginate chain (degree of substitution) was varied from 1 to 20 in these studies. Cell–polymer mixtures were incubated at 37 °C on a shaker to prevent cell sedimentation, and unbound ^{125}I G_4RGDASSKY-alginate molecules were subsequently removed by centrifugation at 1200 rpm for 5 minutes followed by discarding of supernatent. Cells were re-suspended in fresh medium, and bound ^{125}I was measured with a gamma counter. The number of ^{125}I-G_4RGDASSKY-alginate bound to cells was determined as a function of peptide presentation, and parallel studies using the FRET technique were used to calibrated the degree of energy transfer (FRET assay) with absolute numbers of bound ligands (^{125}I-G_4RGDASSKY-alginate studies).

3. Results

The effect of RGD ligand presentation on myoblast proliferation was first investigated by culturing the C2C12 cells or human primary myoblasts on gels comprised of polymers with a varying degree of substitution, presenting peptides with binding affinity, or altering ligand organization. The number of receptor–ligand interactions under these various conditions was next quantified by two independent approaches: rheological measurements and fluorescence resonance energy transfer (FRET) to determine if the effects of ligand presentation on proliferation correlated with bond number.

3.1 Regulation of myoblast phenotype through RGD ligand presentation

The effects of peptide presentation on the immortalized C2C12 cell line were first examined. C2C12 cells were plated on RGD-modified alginate gels, and the initial adhesion and subsequent proliferation rate were dependent on the degree of ligand substitution (Fig. 2A,B). A minimal RGD density was required for cell proliferation, as cells showed very limited spreading and proliferation when RGD was presented at DS 0.2 (Fig. 2A,E). Increasing the RGD density led to faster cell proliferation (Fig. 2E). The decrease in cell number at the DS 20 condition on day 3 was the result of myoblast fusion into multinucleated myotubes, not cell death or detachment (data

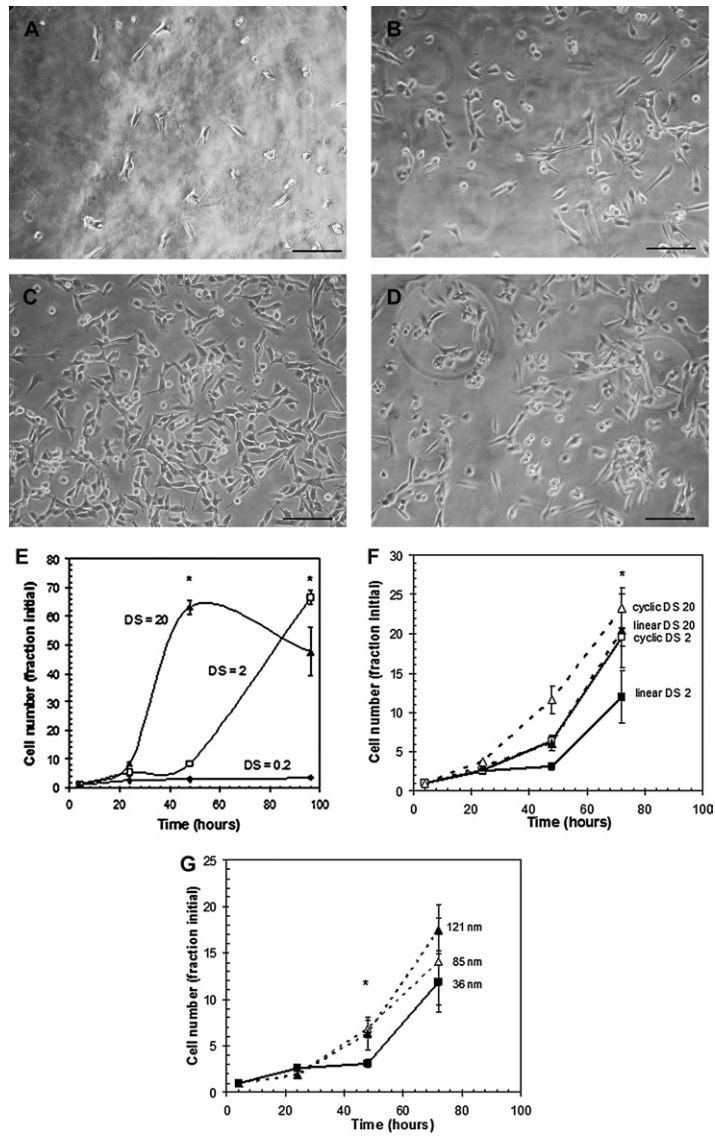

Fig. 2 Photomicrographs of C2C12 myoblasts adherent to alginate gels presenting linear RGD at DS 0.2 (A), linear RGD at DS 2 (B), cyclic RGD at DS 2 (C), and a mixture of polymers coupled with linear RGD and plain polymers at a ratio of 1 : 9 and 1 : 19 (D), which results in a spacing between adhesive islands of 85 nm (20 RGDs/85 nm), 121 nm (40 RGDs/121 nm), respectively, as contrasted to a spacing of 36 nm between polymer chains with ligands when all are labelled (2 RGDs/36 nm) on day 2. The proliferation rate of C2C12 cells cultured on gels varying in DS (E), binding affinity (F), and spacing (G) was determined by cell counts normalized to the initial adherent cell number. Scale bar represents 100 μm (A–D). Values represent mean and standard deviation. * denotes a statistical significance of differences between cell numbers on linear *versus* cyclic peptide conditions, comparing at identical DS (F), and of cell numbers between 2 RGDs/36 nm *versus* 20 RGDs/85 nm and 2 RGDs/36 nm *versus* 40 RGDs/121 nm (G) at each time point (t-test, p-value < 0.05, $n = 4$).

not shown). C2C12 cell growth was also greatly influenced by the binding affinity of the peptide, as the cyclic RGD promoted greater proliferation (Fig. 2C,F) than the linear RGD at the equivalent DS. The nanoscale organization of the RGD ligands was next varied, while maintaining a constant total density of RGD ligands in the gels. C2C12 cells adherent to gels with more clustered RGD peptides demonstrated a more extended shape (Fig. 2D), and significantly higher proliferation, as compared to cells on the gels with uniform RGD distribution (Fig. 2G).

Similar experiments were next performed with human primary myoblasts to determine if they were regulated by peptide presentation in a similar manner. Similarly to the results with the C2C12 cells, the proliferation rate of human primary cells was dependent on the DS of the polymers used to form gels. These primary cells showed

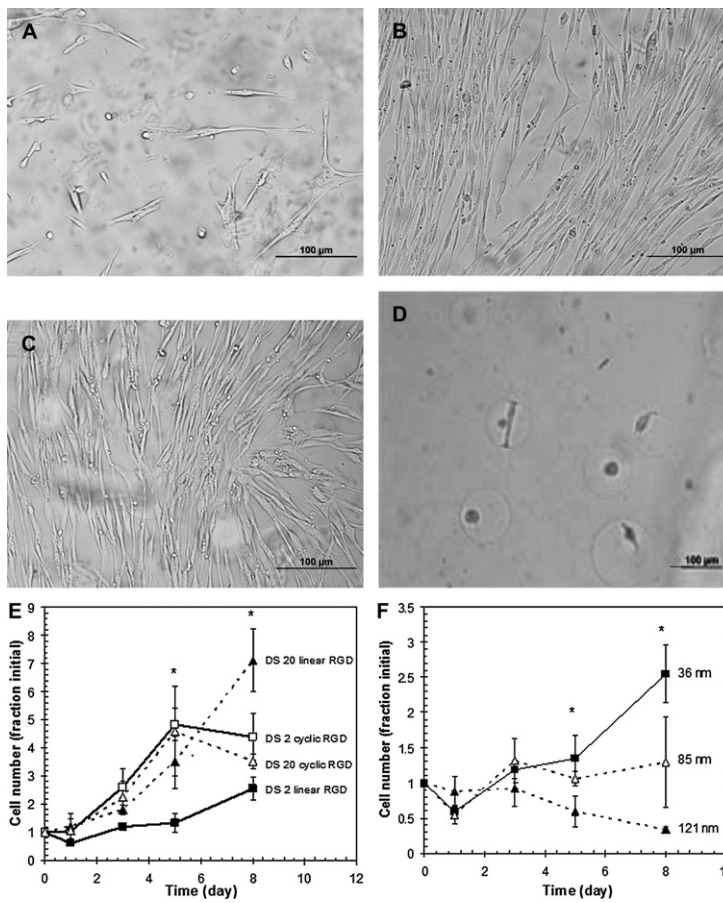

Fig. 3 Photomicrographs at day 8 of human primary myoblasts adherent to alginate gels

presenting linear RGD at DS 2 (A), linear RGD at DS 20 (B), cyclic RGD at DS 2 (C), and a mixture of polymers coupled with linear RGD and plain polymers at a ratio of 1 : 19 (D), which results in 40 RGDs/121 nm, as contrasted to 2 RGDs/36 nm. Proliferation rate of human cells cultured on gels varying in DS and binding affinity (E), and spacing (F) was determined by cell counts normalized by initial adherent cell number. Scale bar represents 100 μm (A–D). Values represent mean and standard deviation. * denotes a statistical significance of differences between cell numbers on linear *versus* cyclic peptide conditions, comparing at identical DS (E), and of cell numbers between 2 RGDs/36 nm *versus* 20 RGDs/85 nm and 2 RGDs/36 nm *versus* 40 RGDs/121 nm (F) at each time point (t-test, p-value < 0.05, $n = 4$).

very slow proliferation on gels presenting linear RGD at DS 2 (Fig. 3A,E). An increase of linear peptide from DS 2 to 20 led to a significant increase in cell proliferation, and cells were able to fuse to form myotubes on day 8 (Fig. 3B) in this condition. This contrasted to cells on the DS 2 condition, as they did not reach confluence, and did not show any cell fusion at this time. The effect of peptide affinity on the proliferation rate of these cells was similar to that found with the C2C12 cells (Fig. 3C,E). However, the results were much more pronounced with human primary cells, especially when comparing at DS 2. An increase of the DS of cyclic RGD from DS 2 to 20 did not further improve human cell proliferation (Fig. 3E). The slight reduction in cell number from day 5 to day 8 was due to cell fusion to form multinucleated cells, not to cell death or detachment (Fig. 3E). The nanoscale distribution of clustered RGD also influenced human primary myoblasts, but strikingly, proliferation was effected in an opposing manner as found with the C2C12 cells. Presenting ligands at a greater spacing and clustered format (20 RGDs/85 nm and 40 RGDs/121 nm) led to significantly lower proliferation, as compared to uniform ligand distribution (2 RGDs/36 nm) (Fig. 3F). The cells adhering to the gels with higher peptide cluster spacing exhibited very limited proliferation, and the cell number actually decreased at 40 RGDs/121 nm. Examination of cell morphology also confirmed these findings, as cells adherent to gels with a uniform peptide distribution were well spread, while the cells adherent to gels with the greater spacing between clustered peptides maintained a round shape (Fig. 3D).

3.2 Quantification of receptor–ligand bond formation with rheological measurements

The number of bonds formed between cell receptors and RGD ligands was next analyzed with rheological measurements to determine if the changes in cell phenotype with peptide presentation directly correlated to the bond number formed in each condition. These measurements are based on changes in the rheological properties of cell–polymer solutions due to cell receptors cross-linking the polymer chains.[20] Non-modified (no peptide) polymer plus cells was first analyzed, and the storage modulus (G') of mixtures was lower than loss modulus (G''), over the entire applied frequency (Fig. 4A), indicating the expected liquid-like property of these mixtures. Strikingly, at the identical cell concentration, the storage modulus (G') of RGD-modified alginate–cell mixtures (DS 20) exceeded the loss modulus (G''), illustrating a transition to a cross-linked network (Fig. 4A). This finding confirmed that cells can act as crosslinking agents by using their receptors to bind with RGD ligands presented from alginate chains, leading to the formation of an ordered structure. This experiment was repeated when cell receptors were first blocked by incubating cells with soluble RGD to confirm the specificity of this gelling process. No solid-like behavior ($G' \ll G''$) was observed when receptors were pre-occupied (Fig. 4B), confirming that network formation was specifically caused by the interactions between cell receptors and RGD ligands coupled to alginate chains. In network formation, multiple cells would be required to crosslink multiple polymer chains, and these interactions would need to percolate through the entire sample volume. By varying the gap size in the plate-plate rheometer, one can test the assumption that this behavior is caused by network behavior, as the time required for percolation should scale with the gap size. Gel-like rheological properties were immediately observed when the gap size was set at 50 μm (Fig. 4C), while it required approximately 25 minutes to establish a network when the gap size was 100 μm (Fig. 4D). Further increasing the gap size to 250 (Fig. 4E) or 1000 μm (data not shown), resulted in no onset of network formation for the observation time frame. However, the disparity between G' and G'' at 250 μm was much less than that of the 1000 μm gap size condition at the end of the first period.

Varying the RGD density dramatically influenced this gelation behavior, as a reduction from DS 20 to DS 2 or 4 decreased the ability of cells to crosslink the

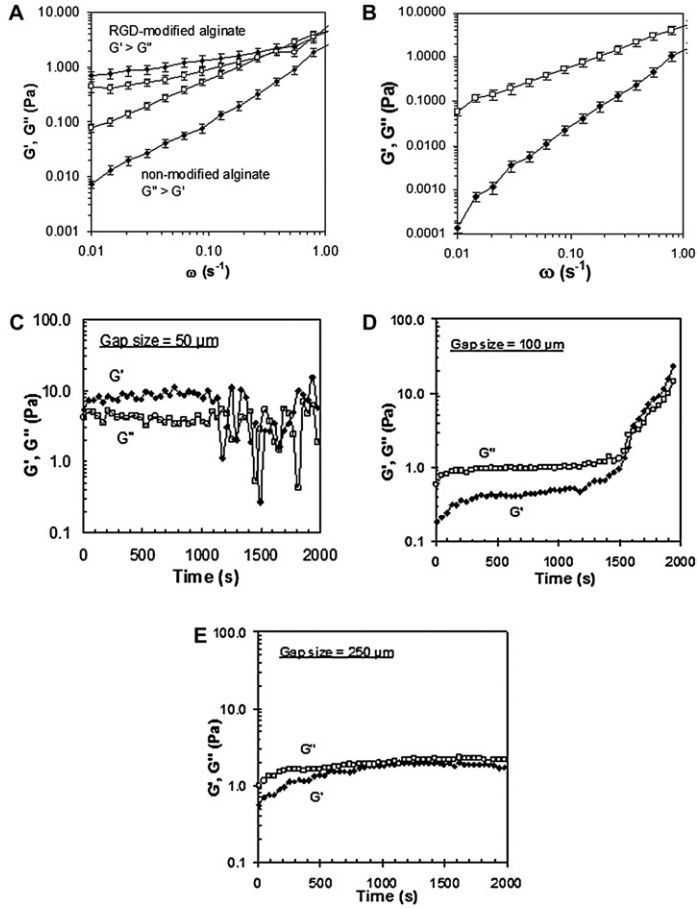

Fig. 4 Storage (G', ■) and loss modulus (G'', □) of cell–polymer mixtures as a function of shearing frequency. A solution of cells with polymer not containing RGD (lower two lines), and linear RGD-modified-alginate–cell solution (upper two lines, DS 20) (A). When the cells were incubated with soluble G_4RGDSP peptides prior to mixing with alginate RGD solution, no network behavior was noted (B). Storage and loss modulus of cell–alginate mixture (RGD DS 20) as a function of time, when the gap size was varied from 50 (C), to 100 (D), and 250 μm (E). Values represent mean and standard deviation calculated from three independent experiments ($n = 3$).

polymers and form gel structures, as indicated by the storage modulus being lower than the loss modulus (Fig. 5A). On the contrary, an increase in DS of RGD from 20 to 40 increased the solid-like property of the mixture (Fig. 5B), as the storage modulus always exceeded the loss modulus, and the difference between G' and G'' was higher at the DS 40 condition ($G' \gg G''$). At the cell concentration used in these studies, a DS at 20 was minimally required to form a gel-like structure. G' and G'' were tested over a large whole frequency range in order to illustrate that the networks fall in the viscoelastic region, and these graphs are provided as supplemental data (data not shown).

The different peptide presentations dramatically influenced network formation. Presenting cyclic RGD from polymer chains greatly enhanced the cell crosslinking behavior, as in this condition at DS 2, a network formed (Fig. 6). An increase of the cyclic RGD density to DS 20 led to an even greater effect, as the magnitudes and difference between G' and G'' were greater (Fig. 6). Presenting RGD peptides

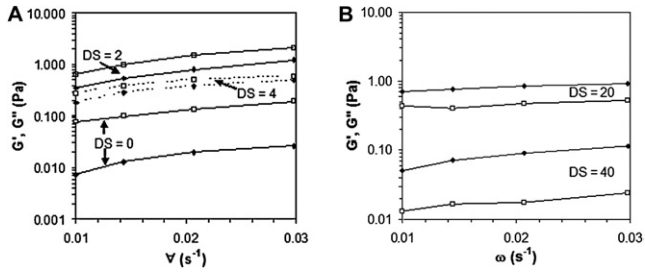

Fig. 5 Storage (G', ■) and loss modulus (G'', □) of cell–polymer mixtures as a function of shearing frequency when polymers were coupled with RGD ligands at varying DS of 0, 2, 4, which behaved with liquid-like property (A), and at DS of 20 and 40, where network formation (solid-like property) was observed (B). The standard deviation for each independent experiment was always less than 15% of its average value ($n = 3$).

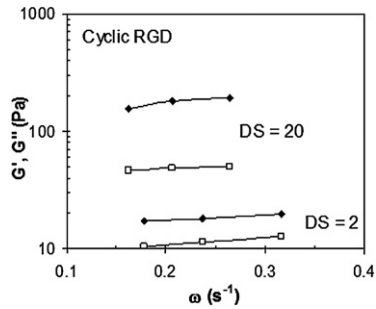

Fig. 6 Storage (G', ■) and loss modulus (G'', □) as a function of shearing frequency for cell–polymer mixtures when were polymers coupled with cyclic RGD at DS 2 and DS 20. The standard deviation for each data point was always less than 15% of its average value ($n = 3$).

in a cluster format also led to network formation, even at an average DS of 4. A uniform distribution of peptide-labeled polymer chains of DS 4 did not lead to network formation (4 RGDs/36 nm) (Fig. 7), but presenting highly clustered RGD peptides (20 RGDs/58 nm or 40 RGDs/85 nm) led to network formation (Fig. 7).

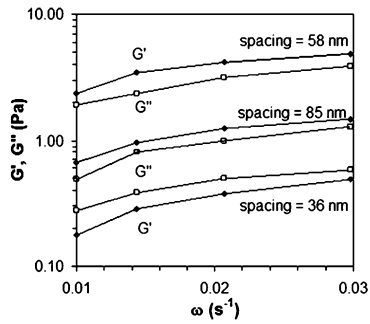

Fig. 7 Storage (G', ■) and loss modulus (G'', □) as a function of shearing frequency for cell–RGD-modified polymer mixtures when RGD ligands were presented at varying RGD spacing, but constant total RGD in the gel (equivalent to uniform presentation of DS 4): uniform distribution resulting in RGD spacing of 36 nm, clustered distribution of mixing DS 20 with unmodified polymers at a 1 : 4 ratio, resulting in RGD spacing of 58 nm (20 RGDs/58 nm), or clustered distribution of mixing DS 40 with unmodified polymers at a ratio of 1 : 9, resulting in an RGD spacing of 85 nm (40 RGDs/85 nm). The standard deviation for each data point was always less than 15% of its average value ($n = 3$).

The temperature dependence of the viscoelastic properties of the cell–alginate mixtures was next determined to quantify the number of cross-links that formed between receptors and RGD ligands. Gels formed with this cell-crosslinking approach displayed higher G' and G'' with a decrease of temperature (Fig. 8A,B). The dependence on temperature was utilized to estimate the zero-shear viscosity, and the horizontal shift factor (a_T), as detailed in the Materials and Methods. The horizontal shift factor could be employed to shift the curves of each temperature to form one master curve, which was a plot between reduced frequency (the product of a_T and frequency) and G' or G'' (Fig. 8C). The activation energy to dissociate cell receptor–RGD interactions per cell was calculated by fitting a_T and $1/T$ with an Arrhenius expression (inserted in Fig. 8C). Available literature values of the force between receptor–ligand per bond ($f_{0,\ \mathrm{linear}} = 3.20 \times 10^{-11}$ N, $f_{0,\ \mathrm{cyclic}} = 4.27 \times 10^{-11}$ N) and bond length ($r_0 = 5$ nm) were used to calculate the number of crosslinks that participated in the formation of the cell-crosslinked structure for varying RGD presentations and DS (Table 1). Increasing the ligand density or binding affinity, and clustering RGD ligands led to an increased number of crosslinks.

A comparison of the growth rate of C2C12 and human primary cells cultured on the various types of gels, and the relative number of bonds formed between cells and these gels indicated an approximately linear correlation between these two measures when the RGD density or binding affinity are increased (Fig. 9), and all of this data for each cell type could be fit by one curve. The relation between proliferation and bond number varied for the two cell types, as the C2C12 cells required many fewer bonds to actively proliferate. Strikingly, results from experiments in which the

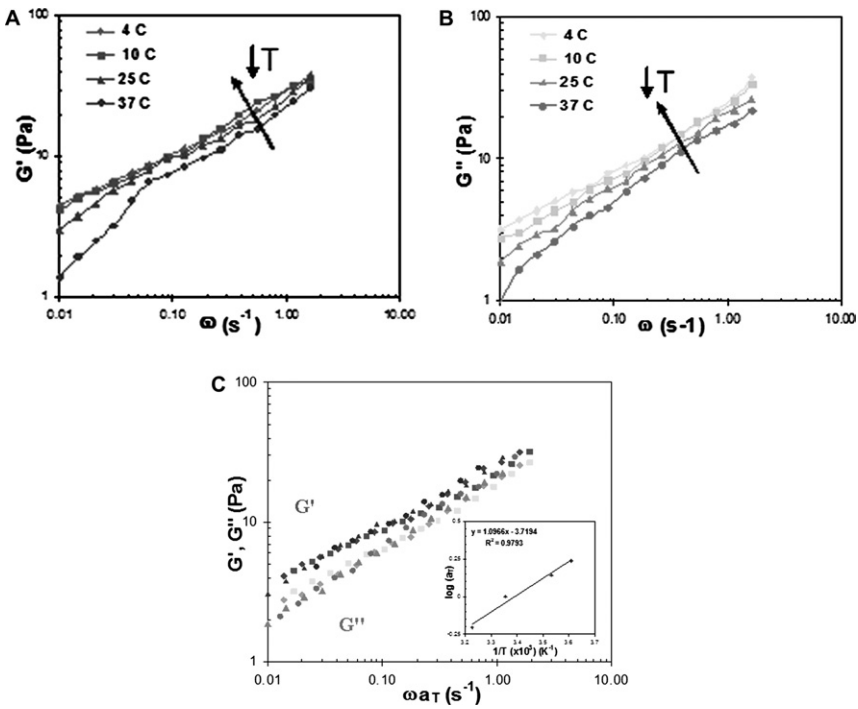

Fig. 8 Temperature dependence of storage (A) and loss modulus (B) of polymer–cell mixture (DS 20, linear RGD as an example). Calculated temperature-dependent shift factor (a_T) was used to superimpose data from multiple temperatures onto a master curve, which was a plot between reduced frequency and storage or loss modulus (C). a_T was plotted *versus* $1/T$ to obtain activation barrier energy (inserted plot in C). The standard deviation for each data point was always less than 15% of its average value ($n = 3$).

Table 1 Summary of calculated activation barrier energy, obtained from slope of plot between log a_T and $1/T$ (for example, inserted plot in 8C), and calculated number of crosslinks between RGD ligand and cell receptors for different RGD ligand presentations

Condition	Average slope (log a_T *vs.* $1/T$)	Calculated activation energy/J	Calculated number of crosslinks/ cell
Linear RGD			
DS = 2	—	—	1
DS = 4	—	—	1
DS = 20	1.0966	3.49 e −20	2.18 ± 0.16
Cyclic RGD			
DS = 2	1.7376	5.52 e −20	2.59 ± 0.12
RGD cluster			
DS 20 : 0 = 1 : 4	1.1278	3.58 e −20	2.24 ± 0.13
DS 40 : 0 = 1 : 9	1.1792	3.75 e −20	2.34 ± 0.13

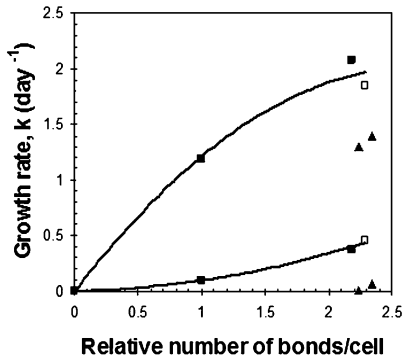

Fig. 9 The correlation between relative number of bonds per cell formed between RGD-containing polymer chains and cells, and the growth rate of the C2C12 cells (upper line) and human primary myoblasts (lower line). The data points arising from experiments in which the DS was changed (■) or ligand affinity was varied (□) all collapsed onto one line. Growth rates (k) were calculated by fitting cell number data to an exponential expression for growth ($N = N_0 2^{kt}$, where N, N_0 = number of cells at time t, and t_0). Data points from experiments in which the island spacing (▲) was varied do not fall on these lines.

nanoscale organizations of RGD ligands were varied did not fall on these curves for either cell type, suggesting the effects of nanoscale ligand organization on proliferation were not simply or solely related to altering bond number.

3.3 FRET measurements to probe receptor–ligand interactions

A FRET technique was next utilized as a completely different and independent means to quantify the interactions between cell receptors and RGD ligands. In this study, cells were labeled with donor fluorophores, while RGD ligands were covalently conjugated with rhodamine as acceptor fluorophores. The dependence of energy transfer on cell density was first determined to obtain the optimal conditions at a constant ligand density (DS 2) for this cell type. The degree of energy transfer was indicated by a reduction of donor intensity at the donor emission wavelength (λ = 520 nm, only cell suspension *versus* cell–RGD modified polymer mixture) when acceptor fluorophore was present (Fig. 10A). A further increase of cell density from 2.5 to 5 million cells per ml led a reduction in the degree of energy transfer, likely due to limited available ligand acceptors, relative to donor fluorophores (Fig. 10B). In contrast, at very low densities (0.5 million cells per ml),

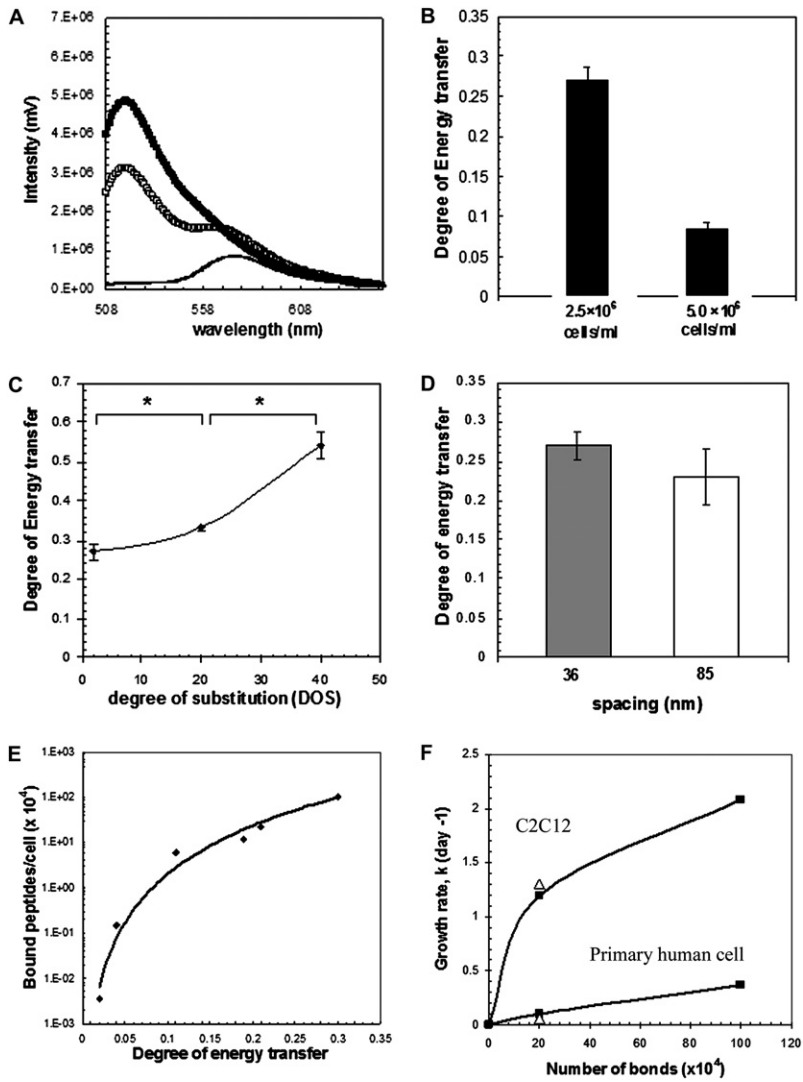

Fig. 10 An example of fluorescent emission intensity of donor fluorophores in the absence (only cell solution, ■), and presence of acceptors (cell–RGD-modified polymer mixtures at DS = 2, □) at total cell concentration of 2.5 million cells per ml. Intensity of acceptor fluorophores (only RGD-modified polymers, —) was measured to account for bleed-through in excitation (A). The degree of energy transfer was determined when cell concentration was varied, while maintaining degree of substitution at 2, and a condition of 2.5 million cells per ml was chosen for other experiments due to the optimal degree of energy transfer (B). The degree of energy transfer was calculated at varying DS (C), and island spacing (D). The correlation between the number of bonds per cell (calculated from the calibration curve between degree of energy transfer and number of ^{125}I-G_4RGDASSKY-alginate bound to cells, (E)) and the growth rate of the C2C12 cells (upper line) and human primary myoblasts (lower line) (F). The data points represent experiments in which the DS was changed (■) or ligand spacing was varied (Δ). Growth rates (k) were calculated by fitting cell number data to an exponential expression for cell growth ($N = N_0 2^{kt}$, where N, N_0 = number of cells at time t, and t_0). * denotes a statistical significance of values between DS 2 and 20, and between DS 20 and 40 (t-test, p-value < 0.05, $n = 4$).

a poor signal to noise ratio precludes obtaining reproducible data. As a result, a density of 2.5 million cells per ml was chosen to test the varying RGD ligand presentations, due to the optimal degree of energy transfer at this concentration. The specificity of the receptor–ligand interactions by this measurement was also confirmed by repeating the experiment when blocking cell receptors with soluble RGD prior to mixing with alginate solutions. Neither a reduction of donor intensity nor any significant energy transfer was found (data not shown). The ligand density significantly influenced the extent of receptor–ligand interactions. An increase of the degree of substitution led to a great reduction of donor intensity, and thus a higher degree of energy transfer (Fig. 10C). This indicated a greater number of interactions between cell receptors and ligands, consistent with the results from the rheological measurements. Varying the ligand distribution, on the other hand, led to no changes in energy transfer at DS 2 (Fig. 10D), in contrast to findings from rheological measurements.

The degree of energy transfer was then calibrated to the absolute number of RGD peptides bound to cells by measuring radiolabeled peptide–alginate binding to cells in solution while performing parallel FRET experiments with cells and soluble RGD–alginate. This calibration curve (Fig. 10E) was utilized to calculate the number of bonds formed between cell receptors and RGD ligands when cells were encapsulated in gels at differing ligand presentations, and to obtain the correlation between the cellular growth rate and the number of bonds measured with FRET (Fig. 10F). Increasing the number of bonds by raising the RGD density resulted in an enhanced growth rate for both cell types, as noted with the rheological assay to monitor bond formation. The relationship between the cell growth rate and the number of bonds formed when RGD ligand affinity was varied also fell on the same curves, although the C2C12 cells again required many fewer bonds to proliferate than the primary cells.

4. Discussion

These data demonstrated how three aspects of RGD presentations—density, affinity and nanoscale distribution—influenced the proliferation of both C2C12 and human primary skeletal muscle cells. There was a minimal required ligand density (DS 2) for cell growth, and increasing ligand density leads to higher proliferation. This is consistent with other studies using several cell types such as osteoblasts,[24] fibroblasts,[33] and endothelial cells.[34] The direct relationship between cell growth rate and bond number, as assessed by FRET and rheological measurements, suggest that varying degree of peptide substitution or affinity effects cell proliferation by regulating bond number. However, the effects of ligand distribution do not appear to be simply related to bond number.

Increasing the ligand affinity through use of cyclic peptides enhanced proliferation of both cell types; although it did not affect initial cell adhesion. Past studies directly comparing linear and cyclic peptides mainly focused in early cellular events, and revealed that increasing the ligand affinity increased neurite extension,[35] fibroblast, smooth muscle and endothelial adhesion,[32,36] and focal adhesion and distribution of fibroblasts.[37] The current results extend the influence of peptide affinity to regulation of proliferation.

The nanoscale organization of RGD ligands regulated spreading and proliferation of both cell types. Interestingly, though, the two cell types had an opposite dependency on ligand distribution. Typically, cell attachment, spreading and proliferation are coherently related (*i.e.*, increased cell spreading leads to increased proliferation) and the results from the C2C12 cells and human primary cells in this study were consistent with this relation.[38] C2C12 cells showed higher initial cell spreading and proliferation when RGD was presented in a clustered format, consistent with studies with fibroblasts on tethered RGDs in a star configuration.[8,39] In contrast, human primary myoblasts demonstrated significantly diminished spreading and

growth on clustered petides. This inhibitory effect of clustering RGD ligands is consistent with a previous study on osteoblast proliferation and differentiation.[24] Previous reports have suggested that an RGD spacing of 140 nm is required for focal contact and stress fiber formation of fibroblasts,[40] but human primary myoblasts may require a spacing less than 121 nm for focal adhesion formation and subsequent promotion of proliferation. Further studies with these and other cell types are needed to delineate the mechanism relating nanoscale peptide organization to cell proliferation, and determine whether the relation is always cell-type dependent.

Rheological measurements and a FRET technique provided extremely useful tools to probe receptor–ligand interactions in this study. As shown by the rheological measurements, classical gel network theory can be exploited to understand these cell–material systems, and enabled us to acquire quantitative information of molecular level interactions. This approach may in the future provide a means for large scale screening to examine the receptor binding ability of other molecules proposed as drugs or cell binding candidates. The rheological measurements, while offering a quantitative assay of bond formation, provided this in relation to the number of crosslinks in the system. The calculated number of crosslinks was very low in all conditions, presumably due to the low probability that a single polymer chain (size scale $\sim$10s of nm) can span between two cells. Brownian motion of cells in the polymer solution likely provides the close proximity required to provide this infrequent cross-linking. The fraction of total polymer–cell bonds resulting in a cross-link may be predicted based on Smoluchowski's equation on cell aggregation.[41] This approach combined with recent Monte Carlo simulations of receptor dynamics[42] may provide a basis to calculate absolute bond numbers from these measurements. In this work, however, a completely independent technique was used to confirm the results from rheological measurements and provide absolute information on bond formation, as previously described.[23]

Higher numbers of bonds were formed between cell receptor and RGD peptides as the RGD density and affinity were increased, as assessed by both rheological and FRET analysis, and bond number in these situations correlated with cell growth rates. This suggests that varying peptide density and affinity may simply regulate cellular function by altering the number of bonds. However, the influence of nanoscale distribution of peptides could not be simply explained by the bond numbers. An increase in the number of bonds was observed when RGD ligands were clustered, as assessed by the rheological measurements, but this did not enhance the C2C12 cell proliferation to the same extent as increasing the number of bonds by increasing ligand density or binding affinity, and actually inhibited the spreading and growth of primary human cells. However, analysis of bond number using the FRET technique indicated a similar extent of bond formation when ligand organization was varied. In either case, though, the proliferation of cells did not correlate well with the clear relation between bond number and proliferation obtained by varying RGD density or affinity. The different bond number measurements with the two assays when peptide clustering/spacing was altered could have a number of causes related to the different conditions used in the measurements. In any case, even if the number of bonds formed is similar between the uniform and clustered peptide distributions, the size of integrin clusters may be different, which could subsequently lead to differing formation of focal adhesions and signaling. Studies examining the relation between RGD distributions and the formation and components of focal adhesions (*e.g.*, vinculin, focal adhesion kinase) may shed light on this issue.

5. Conclusions

Presentation of RGD ligands strongly regulated the proliferation of skeletal muscle cells *in vitro*. An increase in ligand density and affinity led to higher cell proliferation in both primary myoblasts and a cell line. Ligand distribution also regulated the proliferation of both cell types, but in an opposing manner. Rheological measurements

and a FRET technique provided useful tools to quantify receptor–ligand bond formation, and suggest that RGD density and affinity may directly regulate myoblast function by altering the number of bonds formed with the material. This approach to study material–cell interactions provides a highly versatile system that may be broadly applied to other systems and cell types, and to predict cellular function (*e.g.*, proliferation, differentiation) *a priori* based on the number of bonds formed with a material.

6. Acknowledgements

The authors would like to thank the US Army Research Office under contract/grant number DAAD190310168 and the NIH/NICDR (RO1 DE13349) for financial support to the laboratory of D.M., and a Royal King Anantamahidol Scholarship (Thailand) to T.B.

7. References

1 M. D. Pierschbacher and E. Ruoslahti, Cell attachment activity of fibronectin can be duplicated by small synthetic fragments of the molecule, *Nature*, 1984, **309**, 30–33.
2 K. Temming, R. M. Schiffelers, G. Molema and R. J. Kok, RGD-Based strategies for selective delivery of therapeutics and imaging agents to the tumour vasculature, *Drug Resist. Updates*, 2005, **8**, 381.
3 U. Hersel, C. Dahmen and H. Kessler, RGD modified polymers: biomaterials for stimulated cell adhesion and beyond, *Biomaterials*, 2003, **24**, 4385–4415.
4 E. Alsberg, K. W. Anderson, A. Albeiruti, J. A. Rowley and D. J. Mooney, Engineering growing tissues, *Proc. Natl. Acad. Sci. U. S. A.*, 2002, **99**, 12025–12030.
5 J. C. Schense, J. Bloch, P. Aebischer and J. A. Hubbell, Enzymatic incorporation of bioactive peptides into fibrin matrices enhances neurite extension, *Nat. Biotechnol.*, 2000, **18**, 415–419.
6 C. D. Dickinson, B. Veerapandian, X. P. Dai, R. C. Hamlin, N. H. Xuong, E. Ruoslahti and K. R. Ely, Crystal structure of the tenth type III cell adhesion module of human fibronectin, *J. Mol. Biol.*, 1994, **236**, 1079–1092.
7 S. Miyamoto, S. K. Akiyama and K. M. Yamada, Synergistic roles for receptor occupancy and aggregation in integrin transmembrane function, *Science*, 1995, **267**, 883–885.
8 G. Maheshwari, G. Brown, D. A. Lauffenburger, A. Wells and L. G. Griffith, Cell adhesion and motility depend on nanoscale RGD clustering, *J. Cell Sci.*, 2000, **113**, 1677–1686.
9 M. P. Lutolf, F. E. Weber, H. G. Schmoekel, J. C. Schense, T. Kohler, R. Muller and J. A. Hubbell, Repair of bone defects using synthetic mimetics of collagenous extracellular matrices, *Nat. Biotechnol.*, 2003, **21**, 513–518.
10 D. A. Wang, J. Ji, Y. H. Sun, J. C. Shen, L. X. Feng and J. H. Elisseeff, *In situ* immobilization of proteins and RGD peptide on polyurethane surfaces *via* poly(ethyleneoxide) coupling polymers for human endothelial cell growth, *Biomacromolecules*, 2002, **3**, 1286–1295.
11 S. P. Massia and J. Stark, Immobilized RGD peptides on surface-grafted dextran promote biospecific cell attachment, *J. Biomed. Mater. Res.*, 2001, **56**, 390–399.
12 J. A. Rowley, Z. Sun, D. Goldman and D. J. Mooney, Biomaterials to spatially regulate cell fate, *Adv. Mater.*, 2002, **14**, 886–889.
13 R. A. Quirk, W. C. Chan, M. C. Davies, S. J. Tendler and K. M. Shakesheff, Poly(L-lysine)-GRGDS as a biomimetic surface modifier for poly(lactic acid), *Biomaterials*, 2001, **22**, 865–872.
14 A. Pramanik, Ligand–receptor interactions in live cells by fluorescence correlation spectroscopy, *Curr. Pharm. Biotechnol.*, 2004, **5**, 205–212.
15 C. M. Waters, K. C. Oberg, G. Carpenter and K. A. Overholser, Rate constants for binding, dissociation, and internalization of EGF: effect of receptor occupancy and ligand concentration, *Biochemistry*, 1990, **29**, 3563–3569.
16 S. K. Akiyama and K. M. Yamada, The interaction of plasma fibronectin with fibroblastic cells in suspension, *J. Biol. Chem.*, 1985, **260**, 4492–4500.
17 O. Smidrod and G. Skjåk-Bræk, Alginate as immobilization matrix for cells, *Trends Biotechnol.*, 1990, **8**, 71–78.
18 J. A. Rowley, G. Madlambayan and D. J. Mooney, Alginate hydrogels as synthetic extracelllar matrix materials, *Biomaterials*, 1999, **20**, 45–53.

19 A. D. Bach, J. P. Beier, J. Stern-Staeter and R. E. Horch, Skeletal muscle tissue engineering, *J. Cell. Mol. Med.*, 2004, **8**, 413–422.
20 K. Y. Lee, H. J. Kong, L. G. Larson and D. J. Mooney, Hydrogel formation *via* cell crosslinking, *Adv. Mater.*, 2003, **21**, 1828–1832.
21 C. Berney and G. Danuser, FRET or no FRET: a quantitative comparison, *Biophys. J.*, 2003, **84**, 3992–4010.
22 H. J. Kong, T. R. Polte, E. Alsberg and D. J. Mooney, FRET measurements of cell-traction forces and nano-scale clustering of adhesion ligands varied by substrate stiffness, *Proc. Natl. Acad. Sci. U. S. A.*, 2005, **102**, 4300–4305.
23 H. J. Kong, T. Boontheekul and D. J. Mooney, Quantifying the relation between adhesion ligand–receptor bond formation and cell phenotype, *Proc. Natl. Acad. Sci. U. S. A.*, 2006, **103**, 18534–18539.
24 K. Y. Lee, E. Alsberg, S. Hsiong, W. Comisar, J. J. Linderman, R. Ziff and D. J. Mooney, Nanoscale adhesion ligand organization regulates osteoblast proliferation and differentiation, *Nano Lett.*, 2004, **4**, 1501–1506.
25 W. A. Comisar, S. X. Hsiong, H. J. Kong, D. J. Mooney and J. J. Linderman, Multi-scale modeling to predict ligand presentation within RGD nanopatterned hydrogels, *Biomaterials*, 2006, **27**, 2322–2329.
26 C. Powell, J. Shansky, M. Del Tatto, D. E. Forman, J. Hennessey, K. Sullivan, B. A. Zielinski and H. H. Vandenburgh, Tissue-engineered human bioartificial muscles expressing a foreign recombinant protein for gene therapy, *Hum. Gene Ther.*, 1999, **10**(4), 565–577.
27 C. A. Powell, B. L. Smiley, J. Mills and H. H. Vandenburgh, Mechanical stimulation improves tissue-engineered human skeletal muscle, *Am. J. Physiol./Cell. Physiol.*, 2002, **283**(5), C1557–1565.
28 R. G. Larson, *The structure and rheology of complex fluids*. 1999, Oxford, Oxford University Press. pp. 130–131.
29 P. P. Lehenkari and M. A. Horton, Single integrin molecule adhesion forces in intact cells measured by atomic force microscopy, *Biochem. Biophys. Res. Commun.*, 1999, **259**, 645–650.
30 P. P. Lehenkari, G. T. Charras, S. A. Nesbitt and M. A. Horton, New technologies in scanning probe microscopy for studying molecular interactions in cells, *Expert Rev. Mol. Med.*, 2000, **8**, 1–19.
31 G. I. Bell, Models for the specific adhesion of cells to cells, *Science*, 1978, **200**, 618–627.
32 Y. Xiao and G. A. Truskey, Effect of receptor–ligand affinity on the strength of endothelial cell adhesion, *Biophys. J.*, 1996, **71**, 2869–2884.
33 B. T. Houseman and M. Mrksich, The microenvironment of immobilized Arg-Gly-Asp peptides is an important determinant of cell adhesion, *Biomaterials*, 2001, **22**, 943–955.
34 Y. S Lin, S. S. Wang, T. W. Chung, Y. H. Wang, S. H. Chiou, J. J. Hsu, N. K. Chou, K. H. Hsieh and S. H. Chu, Growth of endothelial cells on different concentrations of Gly-Arg-Gly-Asp photochemically grafted in polyethylene glycol modified polyurethane, *Artif. Organs*, 2001, **25**, 617–621.
35 J. C. Schense and J. A. Hubbell, Three-dimensional migration of neurites is mediated by adhesion site density and affinity, *J. Biol. Chem.*, 2000, **275**, 6813–6818.
36 S. P. Massia and J. Stark, Immobilized RGD peptides on surface-grafted dextran promote biospecific cell attachment, *J. Biomed. Mater. Res.*, 2001, **56**, 390–399.
37 M. Kato and M. Mrksich, Using model substrates to study the dependence of focal adhesion formation on the affinity of integrin–ligand complexes, *Biochemistry*, 2004, **43**, 2699–2707.
38 L. K. Hansen, D. J. Mooney, J. P. Vacanti and D. E. Ingber, Integrin binding and cell spreading on extracellular matrix act at different points in the cell cycle to promote hepatocyte growth, *Mol. Biol. Cell*, 1994, **5**, 967–975.
39 L. Y. Koo, D. J. Irvine, A. M. Mayes, D. A. Lauffenburger and L. G. Griffith, Co-regulation of cell adhesion by nanoscale RGD organization and mechanical stimulus, *J. Cell Sci.*, 2002, **115**, 1423–1433.
40 S. P. Massia and J. A. Hubbell, An RGD spacing of 440 nm is sufficient for integrin $\alpha V\beta$ 3-mediated fibroblast spreading and 140 nm for focal contact and stress fiber formation, *J. Cell Biol.*, 1991, **114**, 1089–1100.
41 T. Fukasawa and Y. Adachi, Effect of floc structure on the rate of Brownian coagulation, *J. Colloid Interface Sci.*, 2006, **304**, 115.
42 C. J. Brinkerhoff and J. J. Linderman, Integrin dimerization and ligand organization: key components in integrin clustering for cell adhesion, *Tissue Eng.*, 2005, **11**, 865–876.

